Electronic Supplementary Material (ESI) for Journal of Materials Chemistry A.

Fabrication of a 2.8 V high-performance aqueous flexible fiber-shaped asymmetric micro-supercapacitor based on MnO_2/PEDOT:PSS-reduced graphene oxide nanocomposite grown on carbon fiber electrode

Leila Naderi[a,b], Saeed Shahrokhian[b,c,*], Francesca Soavi[a,*]

[a]Department of Chemistry ‘‘Giacomo Ciamician’’, Alma Mater Studiorum-Universita` di Bologna, Via Selmi 2, 40126, Bologna, Italy

[b]Department of Chemistry, Sharif University of Technology, Tehran 11155−9516, Iran

[c]Institute for Nanoscience and Technology, Sharif University of Technology, Tehran, Iran

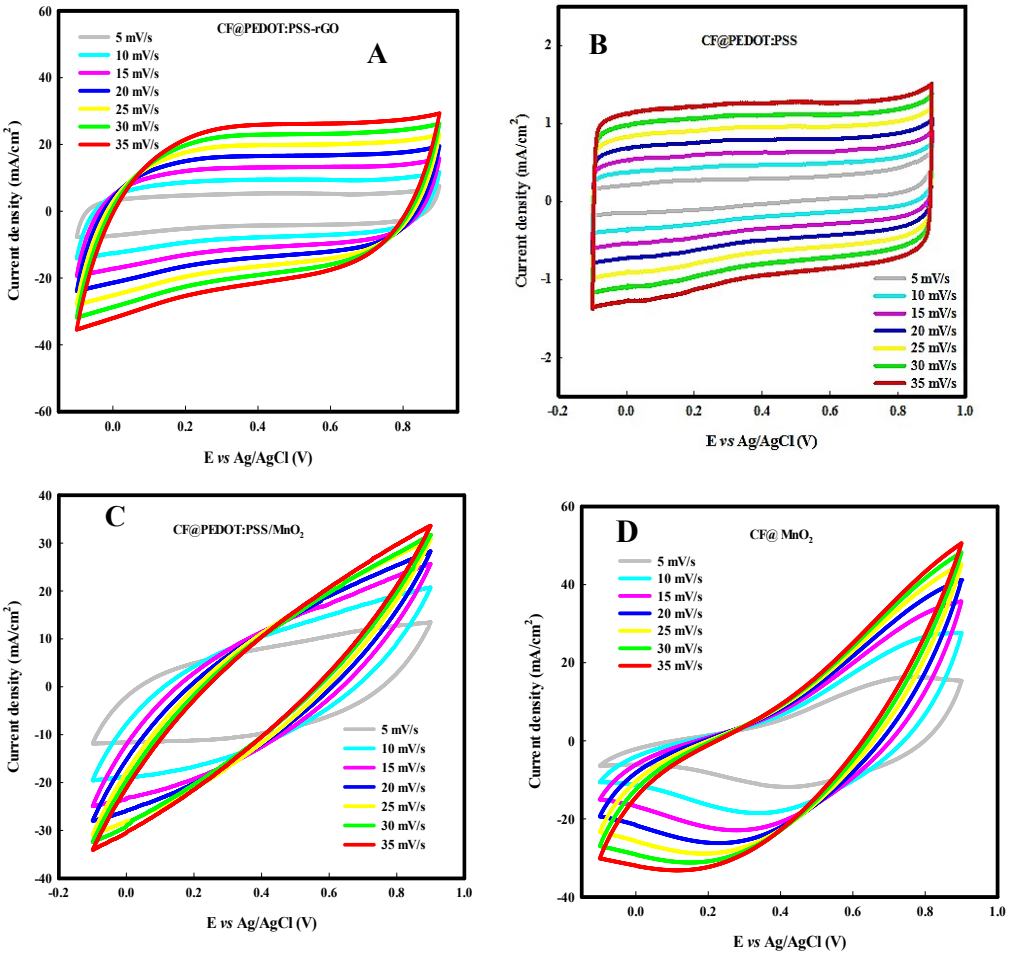

Fig. S1. CV curves of prepared electrodes at different scan rates

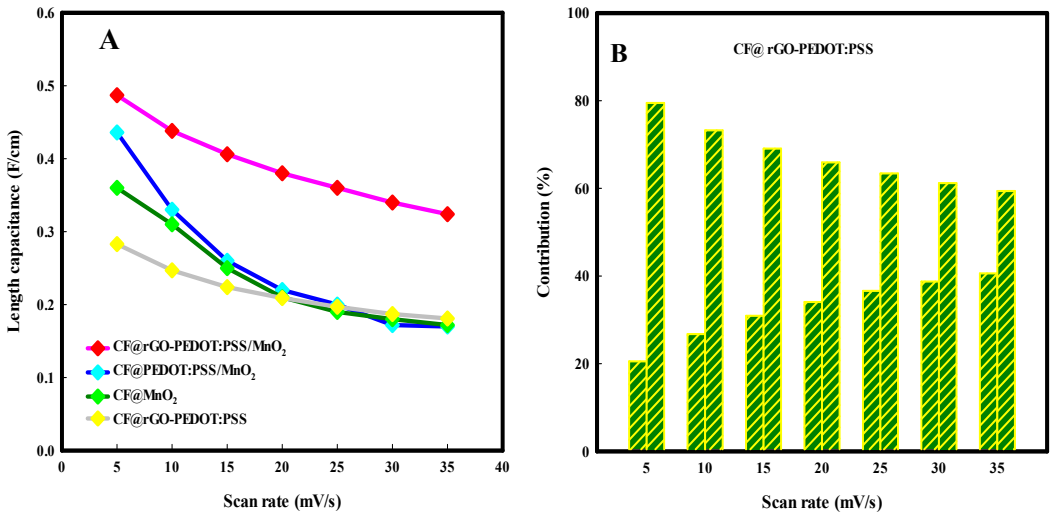

Fig. S2. Length capacitance of the prepared electrodes as function of scan rate (A) Comparison of charge storage for rGO-PEDOT:PSS electrode at different scan rates.

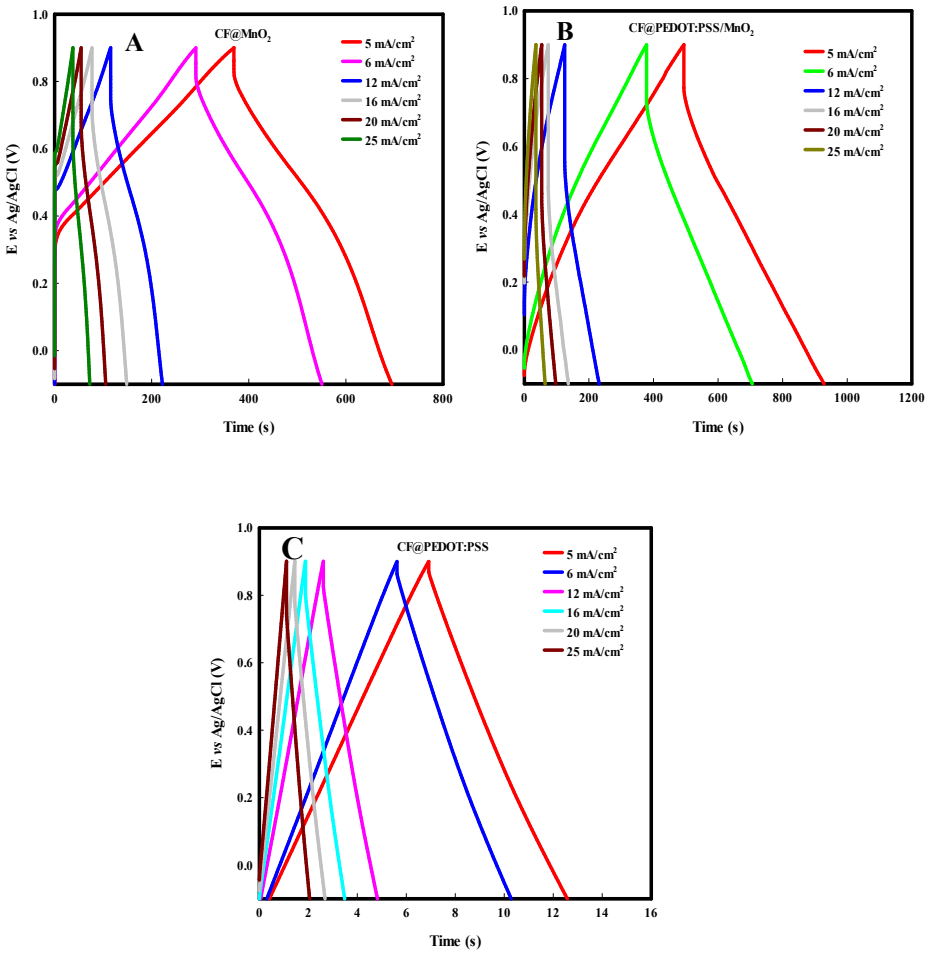

Fig. S3. GCD curves of prepared electrodes at different current densities

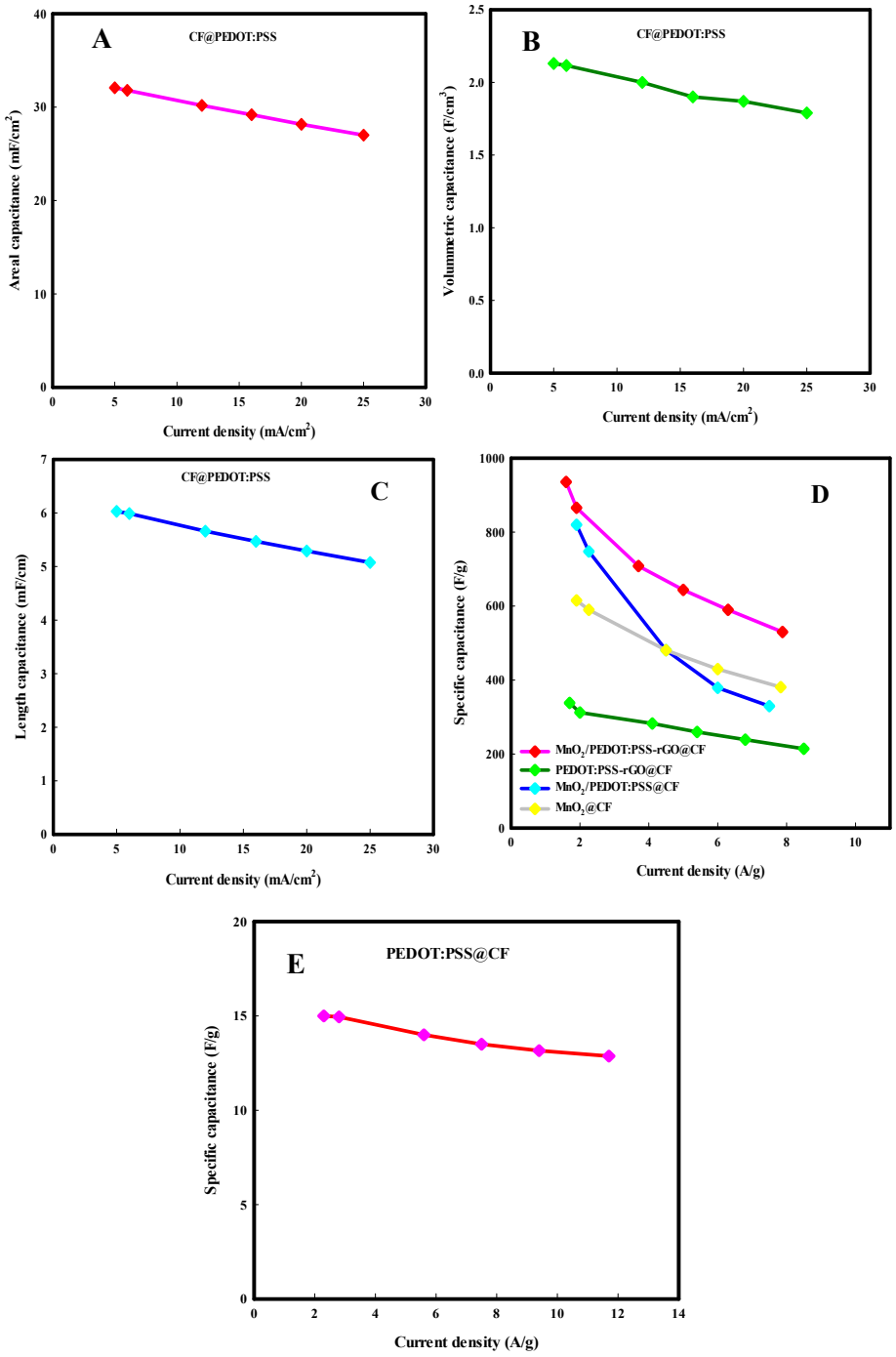

Fig. S4. Areal (A), Volummetric (B) and length capacitance (C) of the PEDOT:PSS@CF as function of scan rate (D, E) Gravimetric capacitance of the different electrodes as function current density

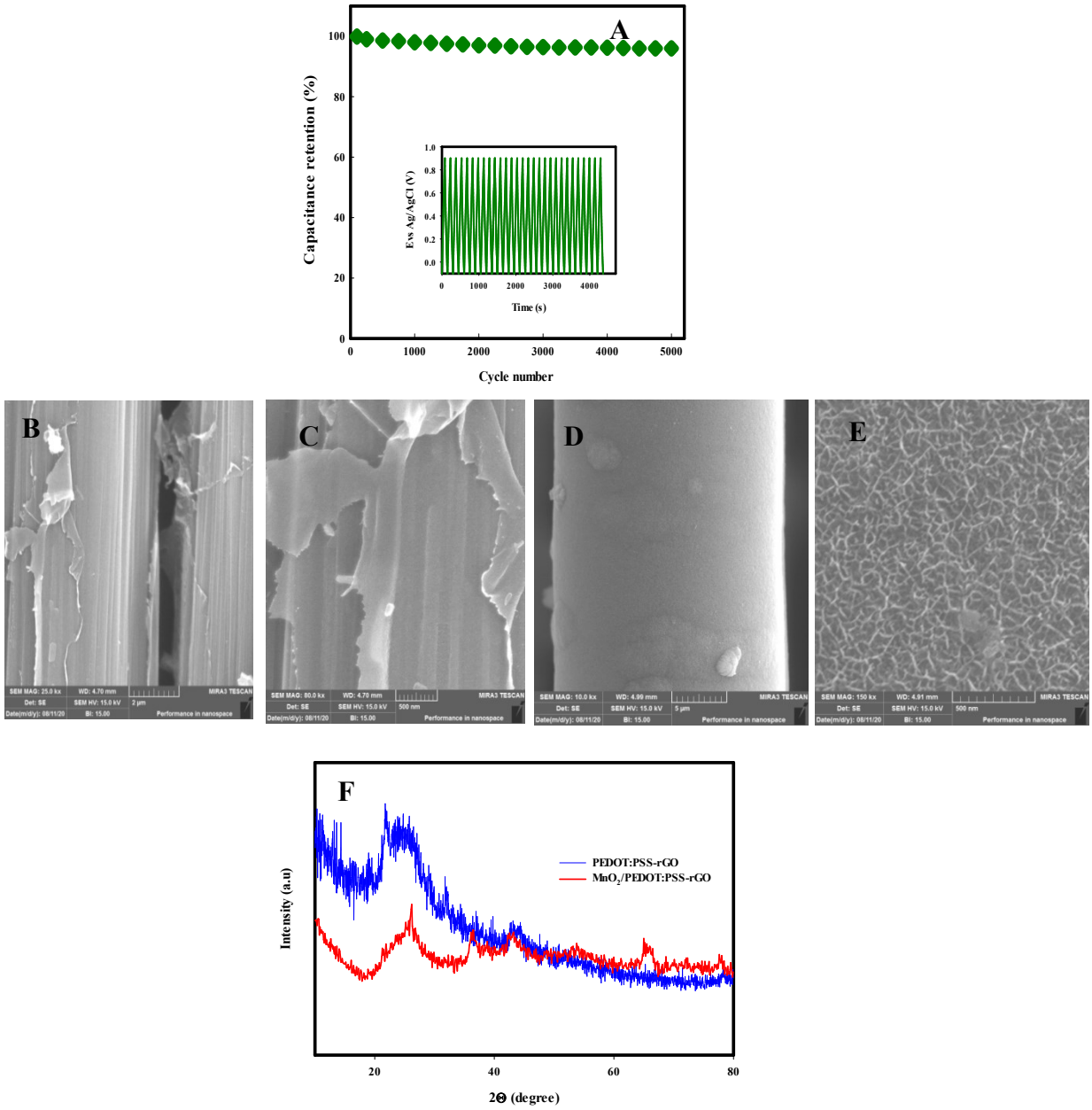

Fig. S5. (A) Long-term cyclic performance PEDOT:PSS-rGO electrode at a current density of 12 mA cm^{-2} (inset: corresponding GCD curves of the last 30 cycles). FE-SEM images of PEDOT:PSS-rGO@CF (B, C), MnO_2/PEDOT:PSS-rGO@CF (D, E) and XRD spectrum of PEDOT:PSS-rGO, MnO_2/PEDOT:PSS-rGO samples after successive cycles (F).

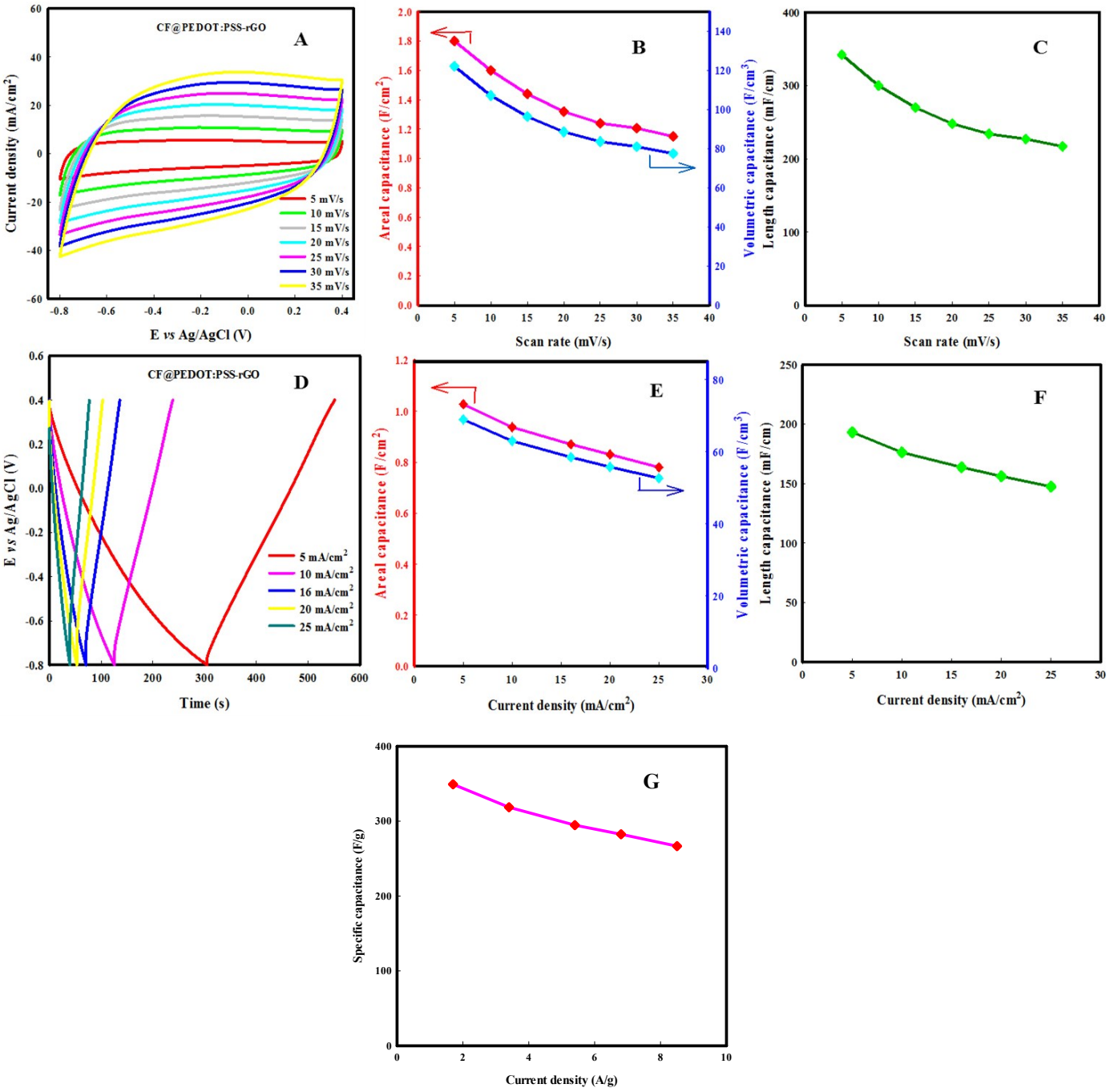

Fig. S6. (A) CV curves of PEDOT:PSS-rGO as negative electrode at different scan rates, (B) Areal and Volumetric and (C) Length specific capacitance of PEDOT:PSS-rGO as a function of scan rate, (D) GCD curves of PEDOT:PSS-rGO at different current densities, (E) Areal and Volumetric , (F) Length and (G) Gravimetric specific capacitance of PEDOT:PSS-rGO as a function of current density

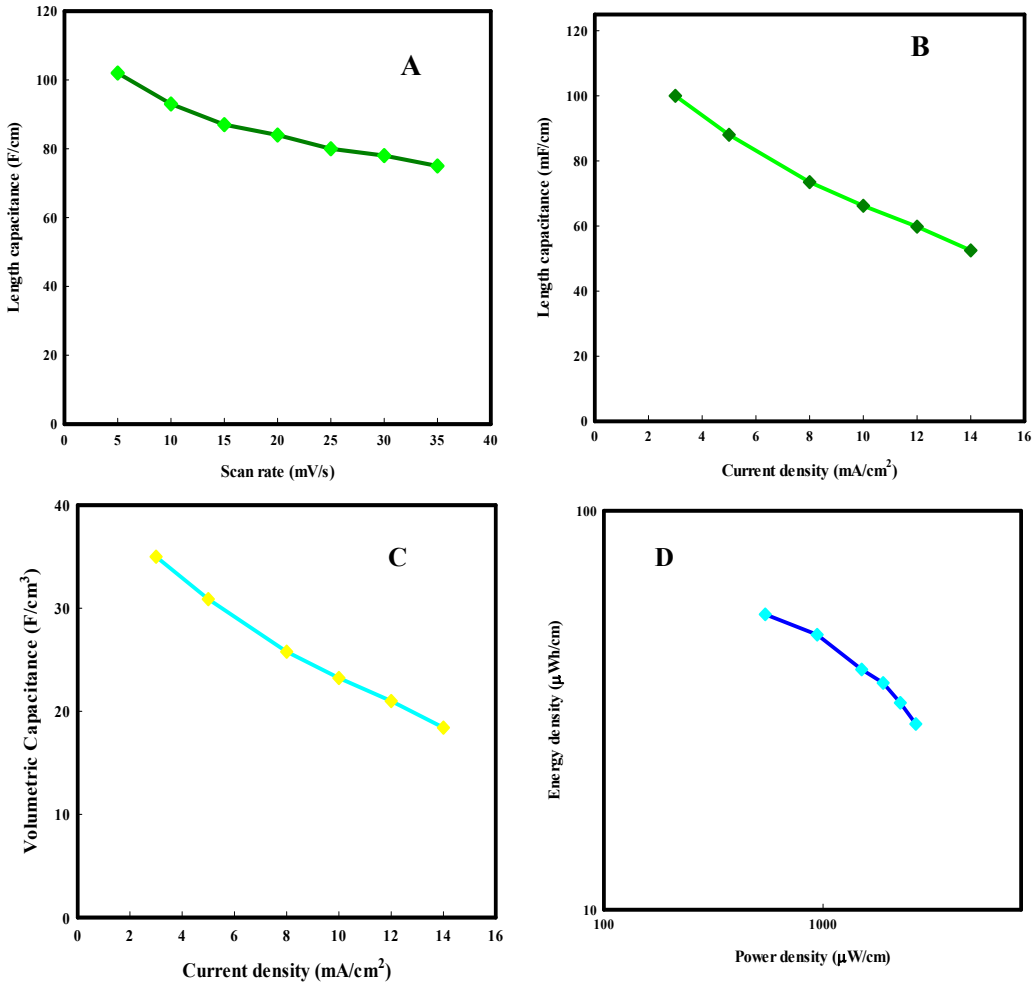

Fig. S7. (A) Length capacitance of the fabricated micro-device as function of scan rate, (B) Length, (C) Volumetric capacitance as function of current density, (D) Length Ragon plot (Na_2SO_4-CMC solid- state electrolyte)

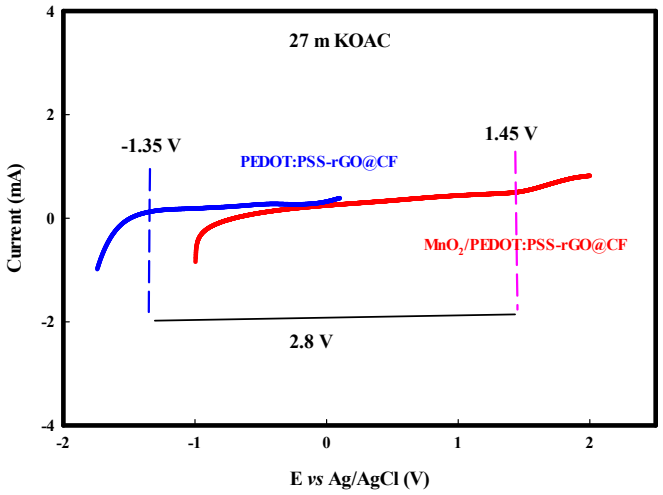

Fig. S8. Linear sweep voltammetry curves recorded at 10 mV/s in 27 m KOAC electrolyte.

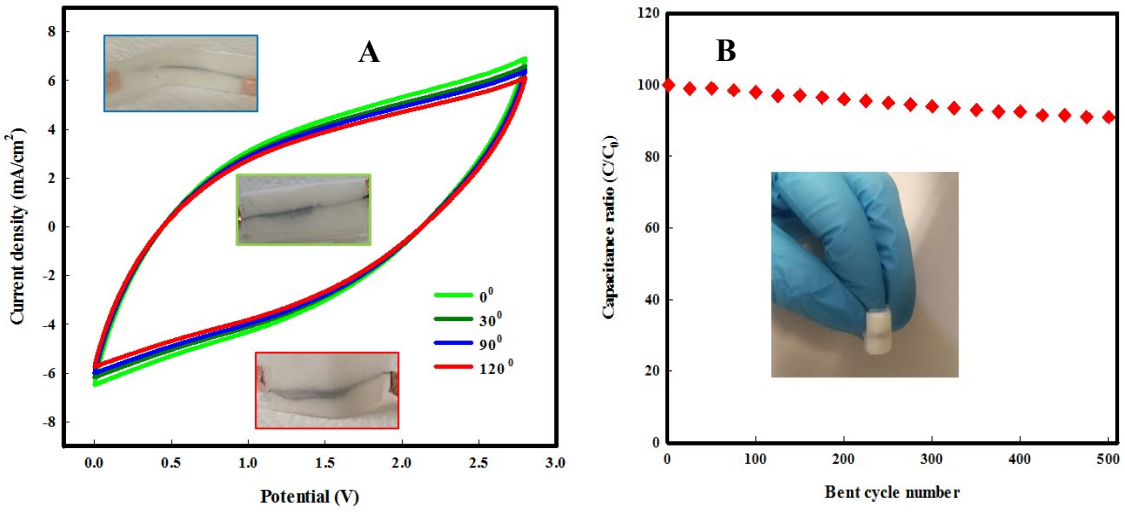

Fig. S9. (A) CV curves of micro- device under straight and different bending states at 35 mV s^{-1}. (B) Dependence of specific capacitance of the micro- device on bent cycle number. (27 m KOAC electrolyte)

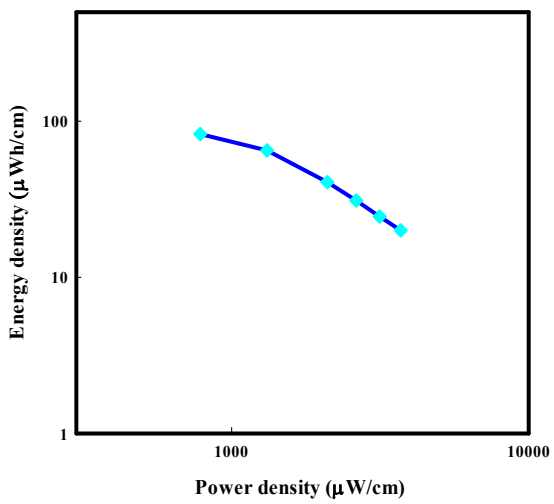

Fig. S10. Length Ragon plot of assembled micro-device in 27m- KOAC electrolyte.

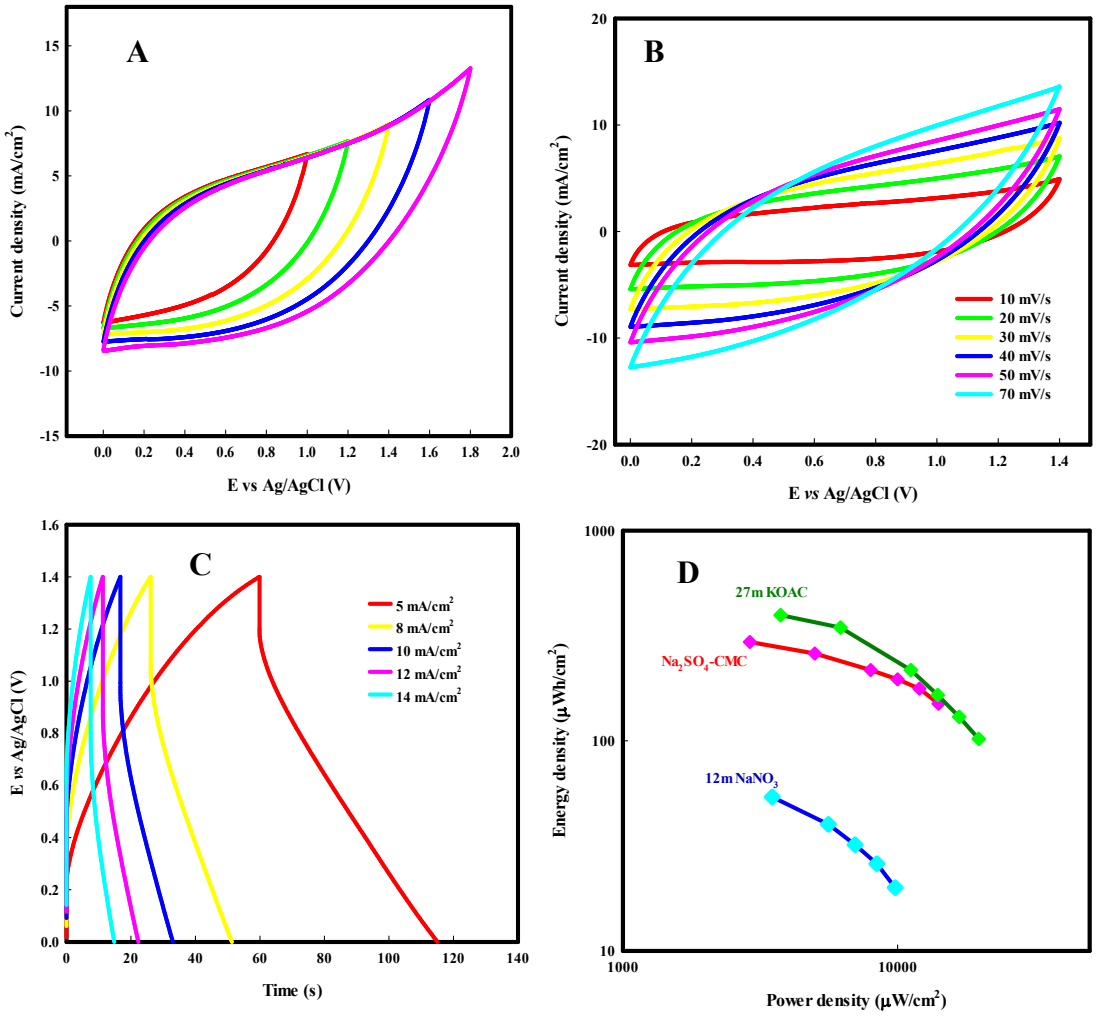

Fig. S11. (A) CV curves of micro-device at different potential windows, (B) CV curves of micro-device at different scan rates in 12 m $NaNO_3$, (C) GCD curves of the micro-device at different current densities. (D) Areal ragon plot of micro-device in Na_2SO_4-CMC, 12 m $NaNO_3$ and 27 m KOAC electrolytes.

Table S1. Comparison of specific capacitances of the present work and other electrode materials in a three-electrode system

Sample	Electrolyte	Specific capacitance	Current density or Scan rate	Voltage window	ref
CF@ PEDOT:PSS-rGO/ MnO_2	1M Na_2SO_4	2920 mF/cm^2 194.25 F/cm^3 549.72 mF/cm	5 mA/cm^2	– 0.1 – 0.9 V	This work
$Ni(OH)_2$/Ni–Cu/ copper wire	NaOH (1M)	12200 mF/cm^2 1220.89 F/cm^3 1530 mF/cm	4 mA/cm^2	0 - 0.55 V	66
CNT/MnO_2 @CF	1M Na_2SO_4	527 F/cm^3	10 mV/s	0 -0.8 V	67
MnO_2/ACF	1M Na_2SO_4	26.64 mF/cm	0.1 mA/cm	0- 1 V	68
CF/MnO_2	KOH	66.4 mF/cm^2	0.5 mA/cm^2	-0.1 – 0.8V	70
PEDOT:PSS/MoO_3	Sulfuric acid	99 F/g 2.99 mF/cm^2	1 mV/s		38
PEDOT:PSS@CuO on Cu foam	3M KOH	907.5 mF/cm^2	3 mA/cm^2	–0.1 – 0.3 V	39
rGO/MoS_2/PEDOT on carbon fiber cloth	1M H_2SO_4	241.81 mF/cm^2	0.5 mA/cm^2	–0.2 – 0.8 V	44
WS_2/PEDOT:PSS Freestanding	1M H_2SO_4	86 mF/cm^2 (411 F/ cm^3)	40 mV/s	–0.3 – 0.5 V	40
PEDOT/Polyaniline Freestanding	H_2SO_4	112.6 F/g	5 mV/s	–0.2 – 0.8 V	41
PPy/PEDOT:PSS@ MWCNT/SF Silk Fabric	1M Na_2SO_4	5296 mF/cm^2	2 mA/ cm^2	–0.4 – 0.6 V	42
Cellulose/PEDOT:PSS/MWCNT	KOH	485 F/g	1 A/g	–0.4 – 0.1 V	43
SWCNT/PEDOT:PSS/CuHcF	1M H_2SO_4	969.8 mF/cm^2	5 mV/s	–0.2 – 0.6 V	62
PANi/PEDOT/PANi/ Ultralarge rgo	1M H_2SO_4	1300 F/cm^3	3 A/cm^3	–0.2 – 0.8 V	45
PEDOT:PSS/MnO_2 Freestanding	0.5 M Na_2SO_4	92.8 F/g	0.1 A/g	0– 0.9 V	47
rGO/MnO_2/PEDOT:PSS binder on nickel foam	1.0 M Na_2SO_4	169.1 F/g	0.1 A/g	0– 1.0 V	46
PEDOT:PSS/MoS_2/PEDOT	1M H_2SO_4	51.01 mF/cm^2 463.73 F/cm^3	0.1 mA/cm^2	–0.2 – 1 V	63
PEDOT:PSS/MnO_2/PEDOT	1 M H_2SO_4	391.36 F/cm^3	3.75 A/cm^3	–0.2 – 1 V	48
MnO_2@PEDOT:PSS@OCNTF	2M LiCl	837.6 mF/cm^2	0.6 mA/cm^2	0– 0.8 V	64
PEDOT:PSS/rGO	1 M H_2SO_4	45.91 F/g	1 A/g	0- 0.8 V	65

Table S2. Electrochemical performances of recent reported supercapacitors

Positive electrode	Negative electrode	Electrolyte	Specific capacitance	Current density	Voltage window	Maximum Energy density	Maximum Power density	ref
CF@ PEDOT:PSS-rGO/ MnO_2	CF@ PEDOT:PSS-rGO	Na_2SO_4–CMC 27m KOAC	550.72 mF/cm^2 100.97 mF/cm 35.43 F/cm^3	3 mA/cm^2	2 V 2.8 V	295.0 µWh/cm^2 55 µWh/cm 19 mWh/cm^3 396.1 µWh/cm^2	14100 µW/cm^2 2650 µW/cm 930.0 mW/cm^3 19740 µW/cm^2	This work
Ni(OH)$_2$/Ni–Cu / copper wire	RGO/ CF	NaOH (1M)	550 mF/cm^2 86 mF/cm 42.3 F/cm^3	3.2 mA/cm^2	1.6 V	195 µWh/cm^2 30.7 µWh/cm 15.04 mWh/ cm^3	7643 µW/cm^2 1200 µW/cm 588.0 mW/cm^3	66
CNT/MnO_2 @CF		PVA/LiCl	91.6 F/cm^3		0.8 V	12.72 m Wh/cm^3	463.8 mW/cm^3	67
CF/MnO_2	CF/MoO_3	PVA/ KOH	4.86 mF/cm^2	0.5 mA/cm^2	2 V	2.7 µWh/cm^2	8.3 mW/cm^2	69
MnO_2/CF		PVA/ NaCl	63 F/g 24 mF/cm		1 V	1.089 µWh/cm	126.65 µW/cm	70
rGO/MoS_2/PEDOT on carbon fiber cloth		PVA/ H_3PO_4	10.35 mF/cm^2	0.104 mA/cm^2	1 V	1.44 µWh/cm^2 at 0.06 mW/cm^2		44
WS_2/PEDOT:PSS Freestanding		H_3PO_4/ PVA	34.5 mF/ cm^2 (86 F/cm^3)	0.4 mA/cm^2	0.6 V			40
PEDOT/Polyaniline Freestanding		PVA/ H_2SO_4	242.5 mF/cm^2 (3.5 F/cm^3)		1 V	0.48 mWh/cm^3	107.14 mW/cm^3	41
PPy/PEDOT:PSS@ MWCNT/SF Silk Fabric	PPy/PEDOT:PSS @ MWCNT/SF	LiCl/PVA	1088.6 mF/cm^2 (13.44 F/cm^3)	2 mA/cm^2	1 V			42
Cellulose/PEDOT:PSS/MWCNT Ni foam	Cellulose/PEDOT:PSS/MWCNT	PVA/ KOH	380 F/g 50.4 F/cm^3	0.25 A/g 0.05 A/cm^3	1 V	13.2 Wh/Kg	0.126 KW/Kg	43
Ag–PEDOT:PSS/ CNT		H_3PO_4 (2 electrode)	64 mF/cm^2 (85.3 F/g)	0.15 mA/cm^2	0.8 V	8.89 µWh/cm^2	0.83 µW/cm^2	76
PEDOT–CNT on Cr/Au		H_2SO_4/ PVA	20.6 mF/cm^2 (82.4 F/cm^3)	0.1 mA/cm^2	1 V	2.82 µWh/cm^2	0.046 W/cm^2	77
SWCNT/PEDOT:PSS/CuHcF	Mo doped WO_3/SWCNT	1M H_2SO_4 (2 electrode)	530.3 mF/cm^2 (100.1 F/cm^3)	10 mV/s	1.4 V	30.08 Wh/L	10.79 kW/L	62
PANi/PEDOT/ PANi/ Ultralarge rgo	PEDOT/ MoS_2	PVA/ H_2SO_4	125 F/ cm^3	3 A/cm^3	0.8 V	5.4 mWh/cm^3	265 mW/cm^3	45
PEDOT:PSS/MoS_2/PEDOT		H_3PO_4/ PVA			1 V	0.2 µWh/cm^2 (1.81mWh/cm^3) under 0.09 mW/cm^3 (0.82 W/cm^3)		63
PEDOT:PSS/ MnO_2/PEDOT		H_3PO_4/ PVA	13.64 F/cm^3	0.2 A/cm^3	1 V			48
MnO_2@PEDOT:PSS@OCNTF		LiCl/PVA	278.6 mF/cm^2	0.6 mA/cm^2	1.8 V	125.37 µWh/cm^2	5400 µW/cm^2	64
PEDOT:PSS/rGO		PVA/H_2SO_4	19.3 mF/cm^2	20 mV/s	0.8 V	2.24 µWh/cm^2	400 µW/cm^2	65